Applications of numerical simulations in built environment.

ASIM, T., MISHRA, R., RODRIGES, S., NSOM, B.

2019

COMADEM
International Journal of Condition Monitoring and Diagnostic Engineering Management

Applications of Numerical Simulations in Built Environment

Taimoor Asim [a]*, Rakesh Mishra [b], Shaun Rodrigues [a], and Blaise Nsom [c]

[a] School of Engineering, Robert Gordon University, Aberdeen, UK (AB10 7GJ)
[b] School of Computing & Engineering, University of Huddersfield, Huddersfield, UK (HD1 3DH)
[c] Université de Bretagne Occidentale, IUT de Brest, IRDL UMR CNRS 6027, France
* Corresponding author. Tel.: +44-1244-262457; email: t.asim@rgu.ac.uk

ABSTRACT

Different types of numerical simulations have been in use for the design and performance analysis of built environment for some time. Most of these simulations are based on simplistic models and methods, such as steady-state approach, which strictly limits the reliability of the predicated results. In the present study, Computational Fluid Dynamics (CFD) based solvers have been used to evaluate the design and performance of a range of built environment applications. The solvers used in the present study have been shown to predict the performance of the built environment with reasonable accuracy, using more realistic modelling techniques. It is expected that the use of CFD for performance analysis of built environment will significantly increase as a result of this study.

Keywords: Computational Fluid Dynamics, Built Environment, Aerodynamics Simulations.

1. Introduction

Accurate performance analysis of the built environment is crucial for efficient and more robust designing. Many researchers have advocated the use of numerical simulations for the performance analysis of built environment [1-3], and many different types of software have been in use for this purpose [4-5]. However, most of these softwares are strictly limited in their modelling approaches. Computational Fluid Dynamics (CFD) based solvers have been proven extensively to be more accurate in the prediction of design and performance analysis parameters [6-10]. Furthermore, CFD based solvers can cater to a wide range of built environment applications such as aerodynamics, aeroacoustics, hydrodynamics etc. [11-15]. There has been a recent increase in the use of CFD in built environment because of multi-purpose nature. This study shows the CFD capabilities in analysing a range of different built environment.

.

2. Modelling Flow Around Buildings

Many different configurations of built environment have been numerically investigated using CFD. For the first investigation, a simple building block has been considered, as shown in figure 1(a). The flow domain has been meshed using polyhedral mesh elements, while the near ground and near-building regions have been meshed using hexehedral mesh elements, with higher mesh density, for accurate prediction of the flow phenomena in the vicinity of the building. The meshing within the flow domain is depicted in figure 1(b).

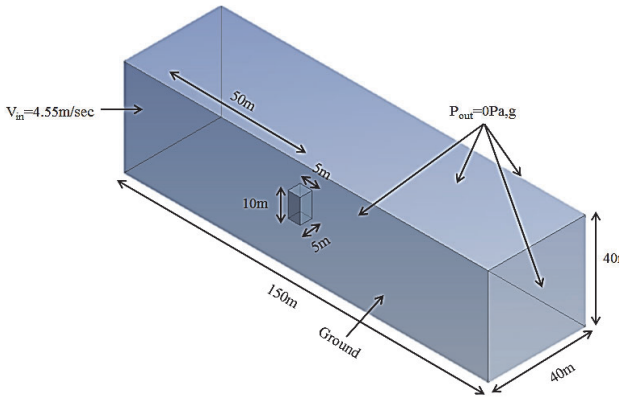

(a)

(b)

Figure 1. (a) A single building block (b) Meshing within the flow domain.

An averaged wind speed of 4.55m/sec in Huddersfield (from Jan 2000 – Dec 2008) has been used as the boundary condition. The predicted static gauge pressure and flow velocity magnitude variations in the vicinity of the building are shown in figure 2. It

can be seen that the static gauge pressure is high at the front of the building, while it is low at the top (due to flow separation). Static gauge pressure recovers almost completely 2h behind the building, where h is the height of the building. Similarly, the flow velocity magnitude can be seen to 0 on the building walls (due to no-slip boundary condition on the walls) and is low in the wake region behind the building. The flow velocity magnitude profiles ahead of the building are shown in figure 3. It can be seen that the presence of the building in the flow domain affects the flow velocity magnitude profiles up to 10m upstream the building. Table 1 summarises the aerodynamic forces acting on the different faces of the building. It can be seen that the front face of the building is subject to maximum drag force of 543N, while the top face of the building is subject to maximum lift force of 237N.

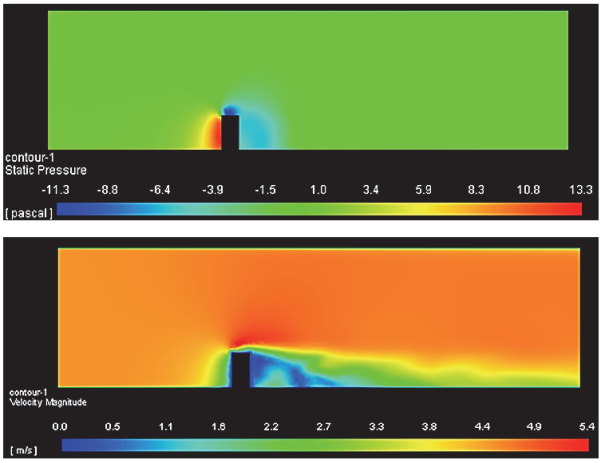

Figure 2. Static gauge pressure and flow velocity magnitude variations in the vicinity of the building.

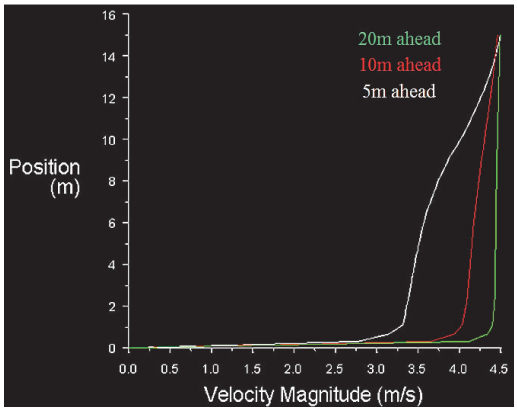

Figure 3. Flow velocity magnitude profiles upstream the building.

Table 1. Aerodynamic forces acting on the different faces of the building.

Face	Drag (N)	Lift (N)	Side (N)
Front	543	0	0
Back	221	0	0
Top	0	237	0
Sides	0	0	37

2.1. Front Shape Effects

It has been shown that the front face of the building experiences the maximum drag force, which in-turn affects its aerodynamic characteristics and structural integrity. Hence, the front face of the building has been modified to curvilinear shapes, as shown in figure 4(a). Figure 4(b) depicts the static gauge pressure variations on the front face of the different building configurations considered. It can be seen that the flow reattachment is enhanced in case of curvilinear configurations, as the static gauge pressure starts recovery on the building faces. Moreover, the maximum static gauge pressure on the curvilinear models is less than on the flat front face model.

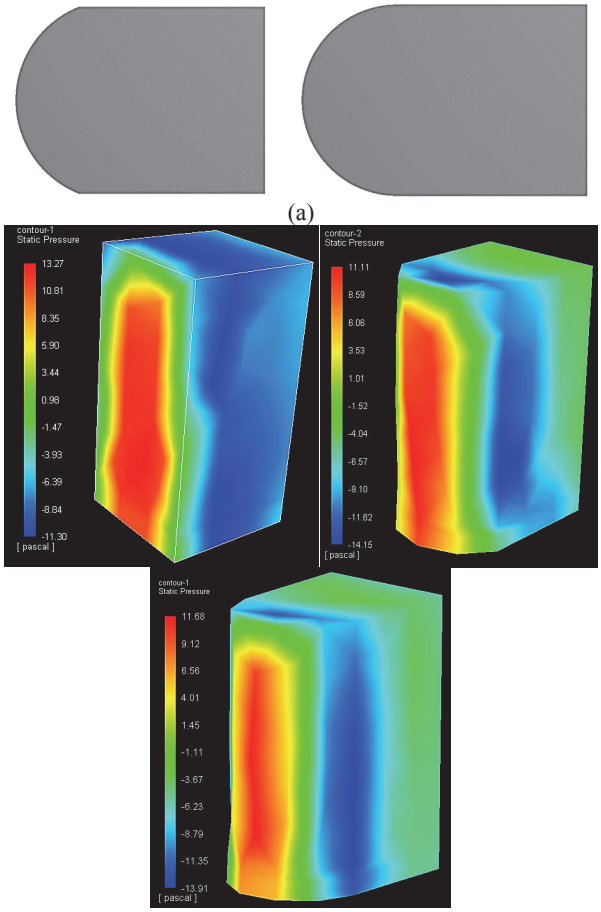

Figure 4. (a) . Curvilinear front faces of the building; Models 1 and 2 (b) Static gauge pressure variations around the different building configurations; Flat front face, Curvilinear Model 1 and Curvilinear Model 2.

Table 2 summarises the aerodynamic forces acting on the different faces of the curvilinear models. It can be seen in comparison with the results presented in table 1 that the front faces of models 1 and 2 experience 62.1% and 74% less drag force as compared to the flat front face model. Similarly, the top faces of models 1 and 2 experience 19% and 21% less lift force as compared to the flat front face model. Hence, the curvilinear building models are aerodynamically more efficient than the flat front face model. Moreover, model 2 is seen to be slightly more efficient than model 1.

Table 2. Aerodynamic forces acting on the different faces of the curvilinear models.

	Face	Drag (N)	Lift (N)	Side (N)
Model 1	Front	206	0	0
	Back	164	0	0
	Top	0	192	0
	Sides	0	0	13
Model 2	Front	141	0	0
	Back	204	0	0
	Top	0	188	0
	Sides	0	0	18

2.2. Skyrise Buildings

Skyrise buildings are a common sight in metropolitans and city centres. Aerodynamic analysis of skyrise buildings is of utmost importance as they significantly affect the aerodynamic behaviour of wind at pedestrian level, and at smaller building blocks. Numerical predictions using simulations is of crucial importance as far as the structural integrity of skyrise buildings is concerned. The skyrise building considered here is uncrowded (no buildings around), with height of 5h, where h is the height of the building block discussed in the previous sections. Figure 5 depicts the static gauge pressure and flow velocity magnitude variations in the vicinity of the skyrise building.

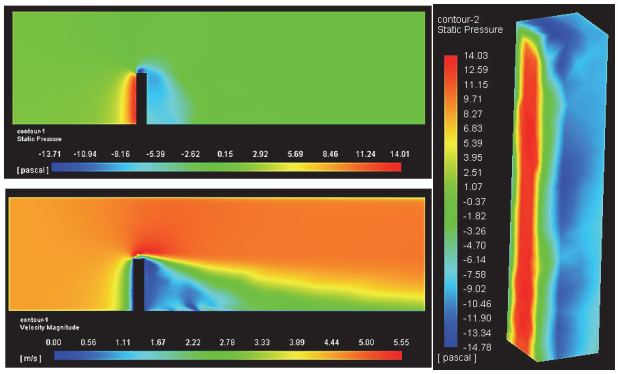

Figure 5. Static gauge pressure and flow velocity magnitude variations in the vicinity of a skyrise building.

It can be seen in figure 5 that the qualitative distribution of the flow variables resembles the one observed in case of a building block earlier, however, the scale of these variations is significantly higher, posing threat to the structural integrity of the building. Table 3 summarises the aerodynamic forces acting on the different faces of the skyrise building. In comparison with the results presented in table 1, it can be seen that the drag force experienced by the front face of the skyrise building is 165.5% higher than for a building block. This is due to the larger area of the front face in case of skyrise building. Moreover, the top face of the skyrise building experiences 22.4% higher lift force than a building block. Hence, the drag force is of more concern to building designers.

Table 3. Aerodynamic forces acting on the different faces of the skyrise building.

Face	**Drag (N)**	**Lift (N)**	**Side (N)**
Front	1442	0	0
Back	782	0	0
Top	0	290	0
Sides	0	0	97

2.3. Crowded Skyrise Buildings

Generally, in metropolitans and city centres, the skyrise buildings are accompanied with standard building blocks. Hence, it is important to analyse the aerodynamic behaviour of the skyrise building in crowded areas. Figure 6 depicts the static gauge pressure and flow velocity magnitude variations in the vicinity of a crowded skyrise building. It can be seen, in comparison with figure 5, that there are significant static pressure and flow velocity non-uniformities at the near-ground level (up to the height of building blocks). These non-uniformities in the flow variables are of significant importance to the designers of skyrise buildings, as well as for the comfort level at pedestrian level.

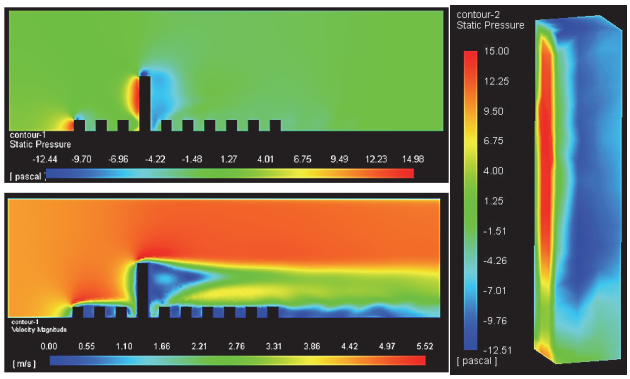

Figure 6. Static gauge pressure and flow velocity magnitude variations in the vicinity of a crowded skyrise building.

Table 4 summarises the aerodynamic forces acting on the different faces of the crowded skyrise building. In comparison with the results presented in table 3, it can be seen that the drag force experienced by the front face of the skyrise building is 11.4% lower than for an uncrowded skyrise building. This is due to the presence of restrictions (building blocks) upstream the skyrise building. Moreover, the top face of the skyrise building also experiences 10.3% reduction in the lift force.

Table 4. Aerodynamic forces acting on the different faces of the crowded skyrise building.

Face	**Drag (N)**	**Lift (N)**	**Side (N)**
Front	1278	0	0
Back	673	0	0
Top	0	260	0
Sides	0	0	9

2.4. Multiple Skyrise Buildings

In metropolitans, it is quite common to have multiple skyrise buildings. In such scenarios, it becomes important to analyse the aerodynamic effects of one skyrise building on the other. Figure 7 depicts the static gauge pressure and flow velocity magnitude variations in the vicinity of the skyrise buildings. It can be seen, in comparison with figure 6, that there are significant static pressure and flow velocity variations as the first skyrise is restricting wind flow to the other skyrise building. Hence, the static pressure variations on the front face of the second skyrise building (downstream) are more uniform as compared to the first (upstream) skyrise building. It is therefore expected that the downstream skyrise building experiences less aerodynamic loads as compared to the upstream skyrise building, which are summarised in table 5.

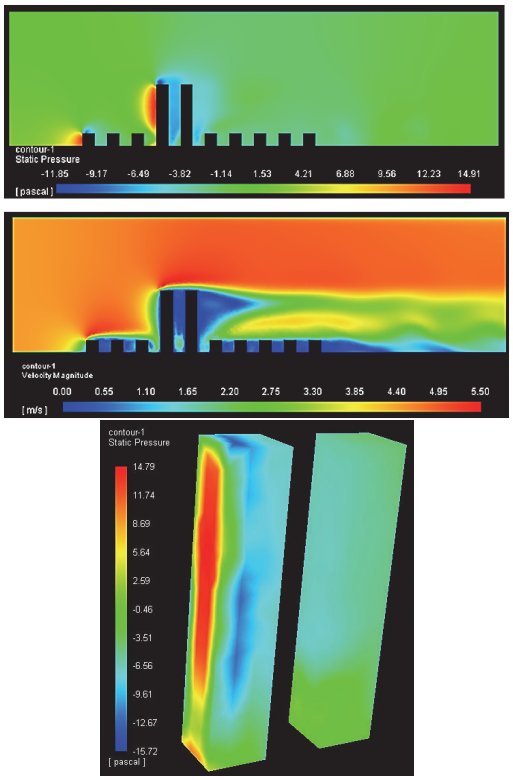

Figure 7. Static gauge pressure and flow velocity magnitude variations in the vicinity of skyrise buildings.

Table 5. Aerodynamic forces acting on the different faces of the skyrise buildings.

	Face	Drag (N)	Lift (N)	Side (N)
Skyrise 1	Front	206	0	0
	Back	164	0	0
	Top	0	192	0
	Sides	0	0	13
Skyrise 2	Front	141	0	0
	Back	204	0	0
	Top	0	188	0
	Sides	0	0	18

2.5. A Practical Example

The aerodynamic behaviour of the University of Huddersfield is presented here. The 50% scaled-down model of the university is shown in figure 8(a). It can be seen that the university comprises of a range of building structures, different in shapes and sizes. The flow domain (figure 8(b)) is a 500m x 500m rectangular block, with a height of 150m. Based on the weather data, averaging from Jan 2000 – Dec 2008, 27% of the winds flow in West direction. Static pressure variations in the vicinity of the university are shown in figure 8(c). It can be seen that the static gauge pressure distribution is highly non-uniform around the university. This information can be useful to the designers for aerodynamically efficient building designs, and pedestrian comfort.

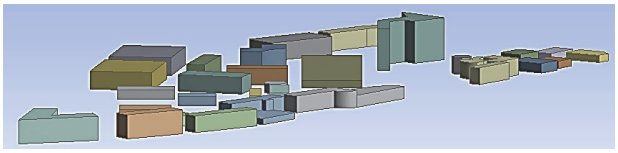

(a)

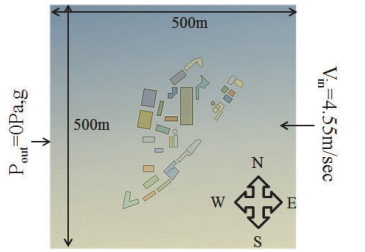

(b)

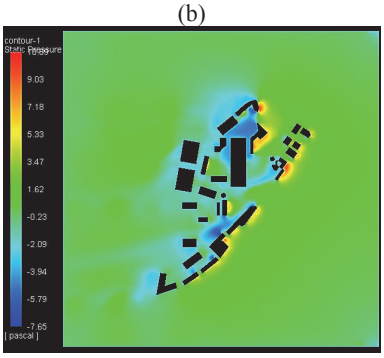

(c)

Figure 8. University of Huddersfield (a) University buildings (b) Flow domain (c) Static gauge pressure variations in the vicinity of the university.

2.6. Gusting Wind Conditions

It is a common practice to design buildings for the maximum aerodynamic loads. Such loads are more pronounced under gusting wind conditions. A common and simplified gust in Huddersfield is shown in figure 9(a), where the wind can accelerate from an average 4.55m/sec to 20m/sec within 10 seconds. Gust effects have been analysed here for the case of a crowded skyrise building. Figure 9(b) depicts the flow velocity magnitude variations at different instances during a wind gust. It can be clearly seen that the wind velocity distribution is highly non-uniform during gusting conditions, ranging from 5.62m/sec to 25.46m/sec, generating significant aerodynamic loading on the buildings, especially the skyrise buildings

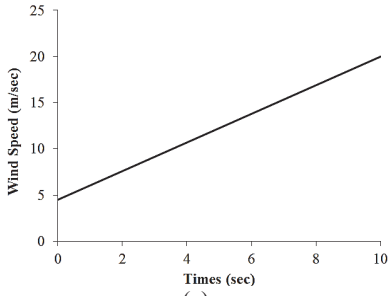

(a)

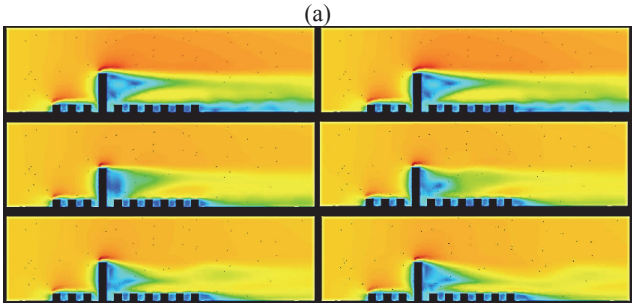

(b)

Figure 9. (a) Gusting conditions in Huddersfield (b) Flow velocity magnitude variations at 0, 2, 4, 6, 8 and 10 seconds.

2.7. CO_2 Emissions

Use of CFD solvers in predicting the emissions behaviour within built environments is very useful in predicting the location and intensity of the emission/s. This has been shown here for the case of a crowded skyrise building with CO_2 emissions from a standard building's roof top. Figure 10 depicts the variations in the volume fraction of CO_2 at various instances during emission. It can be seen that under standard wind speed for Huddersfield (4.55m/sec), CO_2 emissions from the roof top first encounter the restriction from the skyrise building. After getting around the skyrise building, CO_2 flows downstream, however, due to its higher density than air, it flows to the pedestrian level about 5h downstream the skyrise building; h being the height of a building block. Hence, this is the region where the CO_2 concentration is highest, apart from the emissions origin area. This information is helpful in carrying out rescue operations.

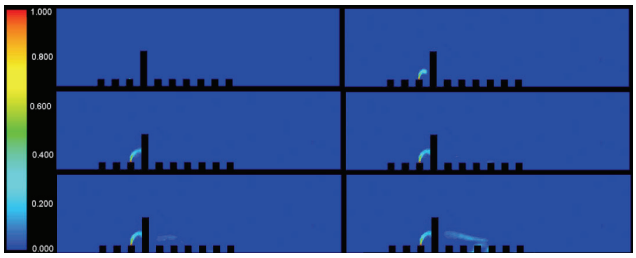

Figure 10. CO_2 volume fraction variations at different instances.

2.7. Flooding

Flooding scenarios can be simulated using numerical simulations, which can provide useful information to the rescue teams. CFD has been used here to simulate flooding in a city centre with a skyrise building. The results presented in figure 11 regarding the variations in the volume fraction of water, at different instances, can be used to carry out effective rescue efforts. It can be seen that first, water flows to the outlet of the flow domain, and then, its level increases in the buildings area.

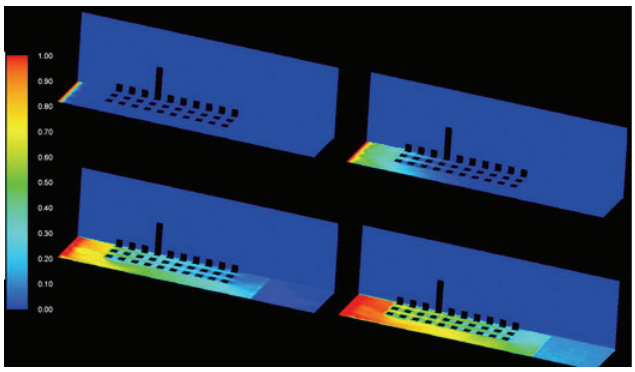

Figure 11. Variations in the volume fraction of water at different instances during a flooding scenario.

A screen system design to predict flooding scenario has also been analysed here (figure 12). This screen system can predict the flow rate of water, indicating the intensity of the flood. Moreover, this system also helps in predicting the water level in different areas under flood. This information can be used to direct rescue efforts in the area under severe threats from the flood.

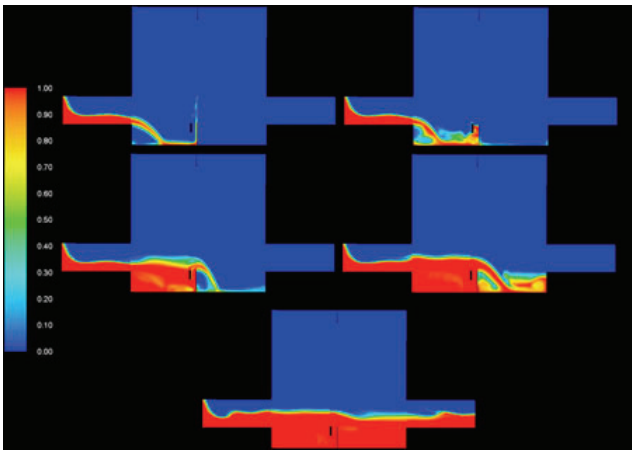

Figure 12. Variations in the volume fraction of water.

3. Modelling Flow Within Buildings

CFD simulations can be used to predict the time dependent variations of temperature within enclosures with reasonable accuracy. A similar study is presented here; figure 13(a-d) shows the flow domain with dimensions. It consists of a radiator at 60^oC, a window that is acting as a sink of $25W/m^2$-K, and a door with its top section acting as an outlet vent at 0^oC while its bottom section acting as air inlet of 0.15m/sec at 20^oC.The manikin is considered to be at 33.7^oC. The static temperature variations within the room, at different instances, are depicted in figure 13(e). It can be seen how the static temperature within the room varies with respect to time. The increase in the room temperature is due to the heat dissipation from the manikin and the radiator. After thermal equilibrium is reached within the room, the static temperature within the flow domain attains an almost constant value.

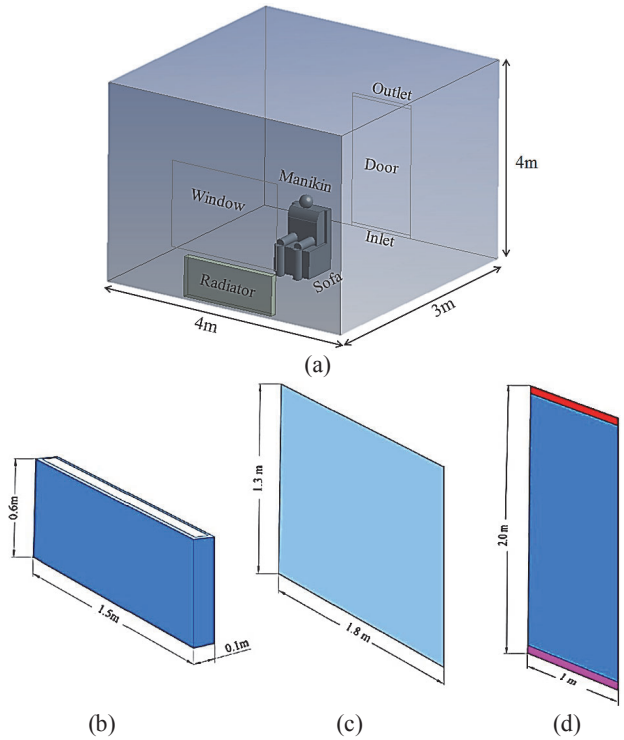

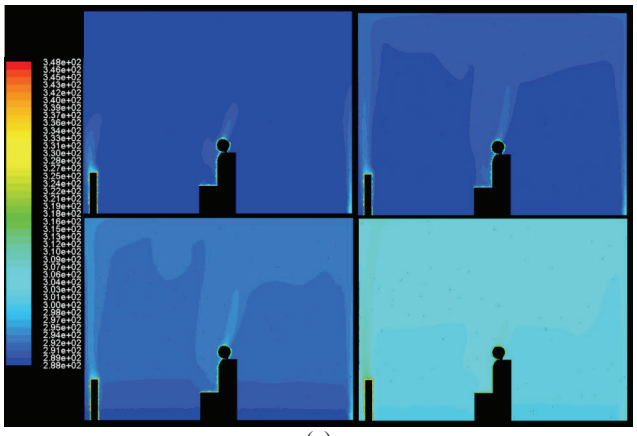

(e)

Figure 13. Room heating (a) Flow domain (b) Radiator (c) Window (d) Door (e) Static temperature variations within the room at different instances.

Another study has been carried out to analyse the effectiveness of a ventilation system in meeting rooms of different geometric configurations (circular Vs rectangular). Using numerical simulations, it is possible to track the air particles, both in space and time, as shown in figure 14. This information, alongwith the particle residence time, can lead to better designs of ventilation systems, as well as enclosures used for public gatherings

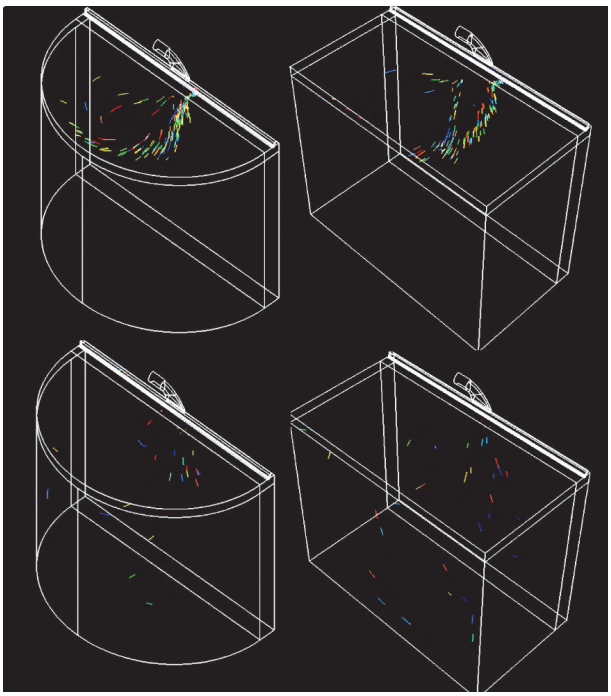

Figure 14. Particle tracking within different enclosures.

4. Conclusions

It has been shown that numerical simulations, and the use of CFD, can be a useful tool in order to analyse a range of different scenarios commonly observed in built environment, such as the aerodynamic behaviour of buildings, contamination and emissions, flooding, heating and ventilation in enclosures, etc. It has been shown that with the increase in the computational power and resources, it has now become possible to analyse not only the flow variables on top of a skyrise building, but also gauge the comfort at pedestrian level in the same simulation, for realistic predictions. Furthermore, accurate predictions from numerical simulations in disastrous situations like emissions and flooding can lead towards better rescue efforts. Using numerical simulations, and CFD solvers, it is possible to accurately predict the temperature variations with enclosures, along with flow patterns that can lead towards more efficient HVAC designs.

References

1. J.A. Clark, Trends in building energy modelling and simulation, Proceedings of the World Renewable Energy Congress IX, 2006.
2. P. Rajagopalan, J.P.C. Wong, M.M. Andamon, Building performance simulation in the built environment education: Experience from teaching two disciplines, Proceedings of the 50th International Conference of the Architectural Science Association, 2016, Adelaide, Australia.
3. K.H. Beattie, I.C. Ward, The advantage of building simulations for building design engineers, 1998.
4. A. Mosavi, Computer design and simulation of built environment; Application to forest planning, Proceedings of the 2nd International Conference on Environmental and Computer Science, 2009, Dubai, UAE.
5. D.B. Crawley, Building performance simulation: A tool for policymaking, PhD Thesis, University of Strathclyde, UK, 2008.
6. T. Asim, Computational fluid dynamics based diagnostics and optimal design of hydraulic capsule pipelines, Ph.D. Thesis, University of Huddersfield, UK, 2013.
7. T. Asim, R. Mishra, Optimal design of hydraulic capsule pipeline transporting spherical capsules, The Canadian Journal of Chemical Engineering, 94 (2016) 966-979.
8. T. Asim, R. Mishra, Computational fluid dynamics based optimal design of hydraulic capsule pipelines transporting cylindrical capsules, International Journal of Powder Technology, 295 (2016) 180-201.
9. T. Asim, R. Mishra, S. Abushaala, A. Jain, Development of a design methodology for hydraulic pipelines carrying rectangular capsules, International Journal of Pressure Vessels and Piping, 146 (2016) 111-128.
10. R. Mishra, S.N. Singh, V. Seshadri, Improved model for the prediction of pressure drop and velocity field in multi-sized particulate slurry flow through horizontal pipes, Powder Handling and Processing, 10 (1198) 279-287.
11. R. Mishra, E. Palmer, J. Fieldhouse, An Optimization Study of a Multiple-Row Pin-Vented Brake Disc to Promote Brake Cooling Using Computational Fluid Dynamics, Proceedings of the Institution of Mechanical Engineers, Part D: Journal of Automobile Engineering, 223 (2009) 865-875.
12. R. Mishra, S.N. Singh, V. Seshadri, Velocity measurement in solid-liquid flows using an impact probe, Flow Measurement and Instrumentation, 8 (1998) 157-165.
13. R. Mishra, S.N. Singh, V. Seshadri, Study of wear characteristics and solid distribution in constant area and erosion-resistant long-radius pipe bends for the flow of multisized particulate slurries, Wear, 217 (1198) 297-306.
14. V.C. Agarwal, R. Mishra, Optimal design of a multi-stage capsule handling multi-phase pipeline, International Journal of Pressure Vessels and Piping, 75 (1998) 27-35.
15. T. Asim, R. Mishra, Large eddy simulation based analysis of complex flow structures within the volute of a vaneless centrifugal pump, Sadhana, 42 (2017) 505-516.